Biotin decorated sunitinib loaded nanostructured lipid carriers for tumor targeted chemotherapy of lung cancer

Somayeh Taymouri[a],*, Maryam Alem[a], Jaleh Varshosaz[a], Mahboobeh Rostami[b], Vajihe Akbari[c], Loghman Firoozpour[d]

[a] Department of Pharmaceutics, School of Pharmacy and Novel Drug Delivery Systems Research Centre, Isfahan University of Medical Sciences, Isfahan, Iran
[b] Department of Medicinal Chemistry, School of Pharmacy, Isfahan University of Medical Sciences, Isfahan, Iran
[c] Department of Pharmaceutical Biotechnology, School of Pharmacy, Isfahan University of Medical Sciences, Isfahan, Iran
[d] Drug Design and Development Research Center, Tehran University of Medical Sciences, Tehran, Iran

ARTICLE INFO

ABSTRACT

Sunitinib (SUN) is an effective and extensively used anticancer agent, but its application is greatly limited by its adverse and undesirable systemic toxic effects. The targeted delivery of SUN could reduce systemic toxicity while maintaining local anti-tumoral efficacy. In this research, a novel nanostructured lipid carrier (NLC) modified with biotin has been designed to overcome this limitation. SUN loaded biotin targeted NLCs (biotin-SUN-NLCs) were prepared by emulsion-solvent diffusion and evaporation method and optimized using irregular factorial design. The morphology of optimized NLCs was studied using SEM. The cytotoxicity of free SUN, SUN-NLCs, and biotin-SUN-NLCs and blank NLCs was evaluated on A549 cells by MTT assay. The optimized formulation presented spherical particle with a mean size of 125.50 nm, 85.10% EE, zeta potential of 10.23 mV, drug release efficiency of about 62.85% during 8 h and PdI < 0.3. Cytotoxicity of biotin-SUN-NLCs was significantly enhanced compared to that of free SUN and SUN-NLCs. The Flow cytometry and fluorescent microscope demonstrated that the biotin-NLCs exhibited higher cellular uptake in A549 human lung cells than non-targeted NLCs. In conclusion, it can be suggested that biotin-SUN-NLCs have advantages and potential for targeted lung cancer therapy.

1. Introduction

Lung cancer is a one of the most leading cause of cancer related death in both primary and metastasis neoplasms. Non-small cell lung cancer (NSCLC) is the most common type of lung cancer and accounts for approximately 85% of lung cancer [1]. The prognosis of lung cancer treated with conventional treatment such as surgical resection, chemotherapy, radiotherapy is unsatisfactory. Most anticancer drugs distribute non-specifically throughout the body and can be harmful to healthy cells, leading to systemic toxicity and severe side effects. Therefore, to minimize side effects the novel, harmless and efficient treatments would be desirable. In the past decade, nano based drug delivery systems (DDS) have been extensively investigated for cancer treatment because nanoparticles (NPs) containing drug not only can increase stability of drugs during their transport in blood circulation but also protect normal tissues from toxicity. NPs can prolong blood circulation time, alter drug biodistribution profile, and allow passive

tumor targeting via enhanced permeability and retention (EPR) effect [2]. Lipid NPs including liposomes, nanostructured lipid carriers (NLCs) and solid lipid nanoparticles (SLNs) are considered as one of the most promising DDS due to bio-acceptable, biodegradable nature of these systems, sustained release behavior, and possibility of production on large industrial scale [3]. NLCs have received growing scientific attention as an improved generation of SLNs to improve cancer treatment. NLCs are composed of solid lipid core along with certain content of liquid lipid (oil) which leads to amorphous state and imperfect lipid structure. Liquid lipids reduce polymorphic transition of solid lipid from disordered crystal structure to ordered crystal lattice resulting in decreasing or preventing common problems associated with SLNs such as drug leakage during storage and limitation in drug loading capacity [3]. Passive targeting is a prerequisite for NPs localization in the tumor interstitium occurs by the EPR effect. To promote uptake of NPs by cancer cells, active targeting can be an effective approach and can be achieved by surface modification of NPs with small targeting ligands

---

such as biotin which widely overexpressed in many cancer cells such as lung cancer [4,5]. Several studies demonstrated that biotin-conjugated drug carriers exhibited high specificity in the receptor-mediated process and significantly increased the cytotoxicity of chemotherapeutic agent. For example, biotin-targeted Pluronic P123/F127 mixed micelles containing niclosamide showed enhanced cytotoxicity against A549 lung cancer cells [4]. SUN is a multi-targeted tyrosine kinase inhibitor with antitumor and anti-angiogenic activities. SUN blocks platelet derived growth factor receptor subtypes and all three vascular endothelial growth factor receptor subtypes (KIT, FLT3, and CSR-1R), glial cell line derived neurotropic factor receptor and colony stimulating factor 1 receptor which have a main role in tumor proliferation, angiogenesis and metastasis [6]. SUN has been successfully investigated for the treatment of imatinib resistant gastrointestinal stromal tumors, advanced renal cell carcinoma and progressive, well-differentiated pancreatic neuroendocrine tumors. Moreover, SUN exhibited clinical activity against NSCLC [7]. However, its application is greatly limited by its adverse and undesirable systemic toxic effects such as, fatigue, nausea, diarrhea, Heart burn, taste changes, severe cutaneous toxicity, hypertension, cardiac disorder, blood clot and low blood count [8]. The targeted delivery of SUN could reduce systemic toxicity while maintaining local anti-tumoral efficacy. Consequently, this study was intended to formulate and optimize a novel targeted NLCs containing SUN. To this end, we conjugated biotin as a target moiety on the stearylamine inserted in NLCs. Then, physicochemical properties such as particle size distribution, zeta potential, surface morphology, encapsulation efficiency (EE), drug release profile, cellular uptake efficiency and cytotoxicity against A549 cells were investigated.

2. Materials and methods

2.1. Materials

SUN base was provided by Parsian Pharmaceutical Co (Iran). Pluronic F127 (PF127), coumarin 6 (C6), biotin, cholesterol (Chol), stearylamine, anhydrous dimethyl sulfoxide (DMSO), 4- N-hydroxysuccinimide (NHS), dicyclohexylcarbodiimide (DCC), and dialysis bag (molecular cut off 12 000 Da) were purchased from Sigma (US). Labrafac was obtained from BASF (Ludwigshafen, Germany). For cell culture study, A549 cell line was provided from Iranian Biological Research Center (Iran). 3-[4,5-dimethylthiazol-2-yl]-2,5-diphenyltetrazolium bromide (MTT) were from Sigma Company (USA). Trypsin, fetal bovine serum (FBS), phosphate buffer saline (PBS), Dulbecco's Modified Eagle Medium (DMEM), penicillin, and streptomycin were purchased from Gibco Laboratories (USA).

2.2. Synthesis of biotin-stearylamine (B-SA) conjugate

B-SA conjugate was synthesized via the reaction of the activated carboxyl group of biotin with the amine group of stearylamine in the presence of DCC and NHS. For this coupling, biotin (700 mg, 2.8 mmol) was dissolved in the anhydrous DMSO. Then, DCC (693 mg, 3.4 mmol) and NHS (387 mg, 3.4 mmol) were added, and the mixture was stirred at room temperature under nitrogen atmosphere for 8 h. The resulting white solid byproduct, dicyclohexylurea, was removed via centrifugation. Then, the supernatant was added dropwise through a syringe to the solution of stearylamine (772 mg, 2.3 mmol) in the anhydrous DMSO. The reaction mixture was stirred for further 24 h at room temperature in the same condition as previous. Finally, the mixture was lyophilized to get the product. The chemical structure of B-SA conjugate was approved using ^{1}H NMR (Bruker, Biospin, AC-400, Mannheim, Germany) and FTIR (WQS-510/520, Raileigh, China) spectra.

2.3. Preparation NLCs

NLCs containing SUN were prepared by the emulsion-solvent diffusion and evaporation method as previously described [9]. The total amount of lipid was employed were 60 mg of which 10% was B-SA conjugate and depending on the formulation code, labrafac was constituted 15% or 30% and Chol made up the remaining 75% or 60% of the lipid. For biotin-SUN-NLCs preparation, the desired amount of Chol, labrafac, B-SA conjugate along with 6 mg or 12 mg of SUN were dissolved into mixed organic solvent of ethanol and acetone (1:1, v/v). Meanwhile, PF127 in concentration 0.5 or 1% w/v was dissolved in 30 mL of distilled water. The two phases were heated separately to the same temperature (at 60 °C). Then, the organic solution was added dropwise using an injection needle into hot aqueous solution of PF127 and stirred with a magnetic stirrer for 5 min at 800 rpm. After the coarse emulsion is formed, the mixture was further sonicated using a probe sonicator (bandelin, Germany) for 2 min at 50 W. In the final step, the obtained nanoemulsion (O/W) was cooled down at room temperature and mixed on magnetic stirrer for 3 h to permit solvent evaporation. To optimize conditions of the technical procedure, irregular full factorial design was employed for preparation of biotin-SUN-NLCs. Four different factors each at 2 levels including lipid/drug ratio (w/w), aqueous/organic phase ratio (v/v), liquid lipid to total lipid ratio (w/w) and surfactant concentration were studied (Table 1). Table 2 illustrates the twelve formulations were investigated. The evaluated response were particle size, polydispersity index (PdI), zeta potential, EE %, release efficiency % during 8 h (RE_8%). The experimental factors and factor levels were chosen on the basis of the result of various initial trials. For the statistical data analysis and determine the contribution effect of each factor, Design Expert software (version 10, US) was used. Analysis of variance (ANOVA) was performed to conclude the significance of the factor and their interaction.

2.4. Characterization of biotin-SUN-NLCs

The mean particle size, PdI, and zeta potential of developed biotin-SUN-NLCs were determined with size/zeta potential analyzer (ZEN 3600 Malvern, U.K) at 25 °C after 5 fold dilution with distilled water. All test performed triplicate.

2.5. Morphology of biotin-SUN-NLCs

Scanning electron microscope (SEM) images were utilized for examining the morphology of NLCs. For this purpose, sample were applied on a metal stubs and then coated with thin layer of gold under argon gas atmosphere. Afterward the samples were analyzed with an upper detector.

2.6. Encapsulation efficiency

For determination of EE of SUN in the NLCs, centrifuge technique was used. 0.5 mL of each biotin-SUN-NLCs formulation was transferred into Amicon microcentrifugation tubes (cutoff 10 000 Da, Ireland) and centrifuged (Microcentrifuge Sigma 30 k, UK) at 14 000 rpm for 10 min.

Table 1
Different factors and their levels investigated by irregular full factorial design in production of biotin modified NLCs loaded with SUN.

Independent variables	levels		Dependent variables
	I	II	
Lipid/drug ratio (w/w)	5	10	Particle size (nm)
Aqueous to organic phase volume ratio (v/v)	5	10	Polydispersity index
Oil content (% total lipid) (w/w)	15	30	Zeta potential (mV)
Surfactant concentration (%)	0.5	1	Encapsulation efficiency (%)
			Release efficiency (%)

Table 2
Composition of different studied biotin modified NLCs loaded with SUN produced by irregular full factorial design.

Formulations	Lipid/drug ratio	Aqueous to organic phase volume ratio	Oil content (% total lipid)	Surfactant concentration (%)
D5O5L15S0.5	5	5	15	0.5
D10O5L15S0.5	10	5	15	0.5
D10O10L15S0.5	10	10	15	0.5
D5O5L30S0.5	5	5	30	0.5
D5O10L30S0.5	5	10	30	0.5
D10O10L30S0.5	10	10	30	0.5
D5O10L15S1	5	10	15	1
D10O5L15S1	10	5	15	1
D10O10L15S1	10	10	15	1
D5O5L30S1	5	5	30	1
D5O10L30S1	5	10	30	1
D10O5L30S1	10	5	30	1

D: Lipid/Drug ratio O: Aqueous/organic phase ratio L: Labrafac/lipid ratio S: Pluronic F127 (%).

The un-encapsulated drug in supernatant was determined by measuring the UV absorbance at 432 nm using a UV-VIS spectrophotometer. After calculating the quantity of free drug, the drug EE in the NPs were determined using following equations:

$$EE = \left(\frac{total\ amount\ of\ drug\ added - free\ drug}{total\ amount\ of\ drug\ added} \right) \times 100 \qquad (1)$$

2.7. In vitro drug release

The *in vitro* release study was carried out using dialysis method. Briefly, the appropriate amount of drug-loaded NLCs were placed in a dialysis bag (molecular cut off 12 000 Da, Sigma, US.) which were sealed at both the ends and dialyzed against PBS (pH 7.4) containing 0.1% Tween 80 to provide sink condition. At predefined intervals, 1 mL of receiving buffer solution was withdrawn and replaced with equal volume of fresh PBS. Finally, the amount of SUN released was determined at 432 nm by a UV spectrophotometer. The parameter of $RE_8\%$ was used to compare release profile and calculated by equation (2):

$$RE_8\ \% = \frac{\int_0^t y.\ dt}{y100.t} \times 100 \qquad (2)$$

Where y is the released percent at time t.

2.8. Cell viability assay

The cytotoxicity of free SUN, SUN-NLCs, and biotin-SUN-NLCs and blank NLCs was evaluated on A549 cells by MTT assay. The cells were seeded at a density of 5×10^3 cells/well in 96-well plates. After 24 h of incubation, they were incubated with different samples at the equivalent SUN concentrations varying from 0.5 to 4 μg/mL for 48 h. At the end of incubation time, MTT solution (20 μl, 5mg/ml) was added to each well, and the cells were incubated for another 4 h at 37 °C. Then, the medium was removed, and 150 μl of DMSO was added to each well to dissolve formazan crystals. The absorbance at 570 nm was measured using a microplate reader. Finally, the cell viability % was determined using equation (3). The cells treated with the same amount of PBS were taken as the negative control and the blank culture medium was used as the control. The statistical analysis of data was done using ANOVA by STATISTICA 18 (Statsoft1, Inc.) software.

$$Cell\ viability\%$$
$$= \frac{Mean\ absorbance\ of\ sample - mean\ absorbance\ of\ blank}{Mean\ absorbance\ of\ control - mean\ absorbance\ of\ blank}$$
$$\times 100 \qquad (3)$$

2.9. In vitro cellular uptake study

C6 as a fluorescent probe was loaded into the targeted and non-targeted NLCs and the cellular uptake was studied via fluorescence microscope (CETI, Belgium) and flow cytometry (BD FACSCalibur, US). The fluorescent NLCs were prepared in a same way as the NLCs loaded with SUN, except SUN was replaced with 1 mg of C6. For flow cytometry study, A549 cells were seeded in 12 well plates at the density of 2.5×10^5 per well and incubated overnight. After that, the cells were treated with 200 ng/ml of C6 -NLCs or biotin-C6-NLCs at 37 °C for 3 h. Subsequently, cells were washed three times with PBS, trypsinized, and resuspended in PBS. Then, resulting cell suspension was analyzed by flow cytometer.

For fluorescent microscopy study, A549 cells were seeded in 96 well plates at the density of 2×10^4 per well and incubated at 37 °C for 24 h. After 3 h incubation of cells with C6 -NLCs or biotin-C6-NLCs, cells were washed three times with PBS, and then the cell monolayer was imaged with fluorescent microscope.

3. Results and discussions

3.1. Synthesis and characterization of B-SA conjugate

The B-SA conjugate was successfully obtained in 71.8% yield. The structure of B-SA conjugate was confirmed by ^{1}H NMR and FTIR spectra. Fig. 1 shows the ^{1}H NMR spectra of biotin, stearylamine and B-SA conjugate in DMSO-d_6. The proton assignment of B-SA conjugate is as follows: σ (ppm): 0.9 (terminal methyl group of stearylamine), 1.2–1.7 (CH2, alkyl chain of stearylamine and H_I, H_J and H_K of biotin together), 2.1 (H_H), 2.6 ($H_{G'}$), 2.9 (H_G), 3.1 (CH2 of stearylamine next to the amide group), 3.2 (H_F), 4.2 (H_E), 4.4 (H_D), 6.4–6.6 (H_B and H_C), 7.9 (H_A). Due to the amide bond formation bonding between the amine group of stearylamine and the carboxyl group of biotin, the H_H (2.2 ppm) of biotin which is next to the carboxyl group, has appeared with a little up-field displacement (2.1 ppm). The CH2 group of stearylamine, next to the amide group, has appeared almost in down field (3.1 ppm) compared to the corresponding peak in stearylamine spectrum (2.6 ppm). Also, the signal related to the carboxylic proton of biotin (Fig. 1 A) in 12 ppm, was completely disappeared after the conjugation with stearylamine (Fig. 1C). These spectral results are indicated that stearylamine and biotin are covalently bonded to each other. Fig. 2 shows the FTIR spectra of biotin, stearylamine, and B-SA conjugate. In the FTIR spectrum of B-SA conjugate, we see the characteristic absorption bands at 3306.36 cm^{-1} (N-H str.), 2922 and 2851.24 cm^{-1} (aliphatic C-H str.), 1699.94 cm-1 (C=O str. of amide group), 1644.02 cm^{-1} (C=O, biotin residue) along with the other specific bands for both of biotin and stearyl amine in the remaining area of the spectrum. As we can see in Fig. 2 A, the absorption band of COOH group in biotin at 1711 cm^{-1} was disappeared in the spectrum of product due to chemical bonding between the amine of stearyl amine and the carboxyl group of biotin. Furthermore, a newly absorption band around 1699.94 cm^{-1} (Fig. 2C) confirmed the amide bond between biotin and stearyl amine. We measured degree of biotin conjugation to stearylamine using the relative integral ratio of signals at 7.9 ppm for stearylamine and 6.6 ppm for Biotin. The integral intensities reveal the 1:1 conjugating ratio for this reaction.

3.2. Characteristics of NLCs

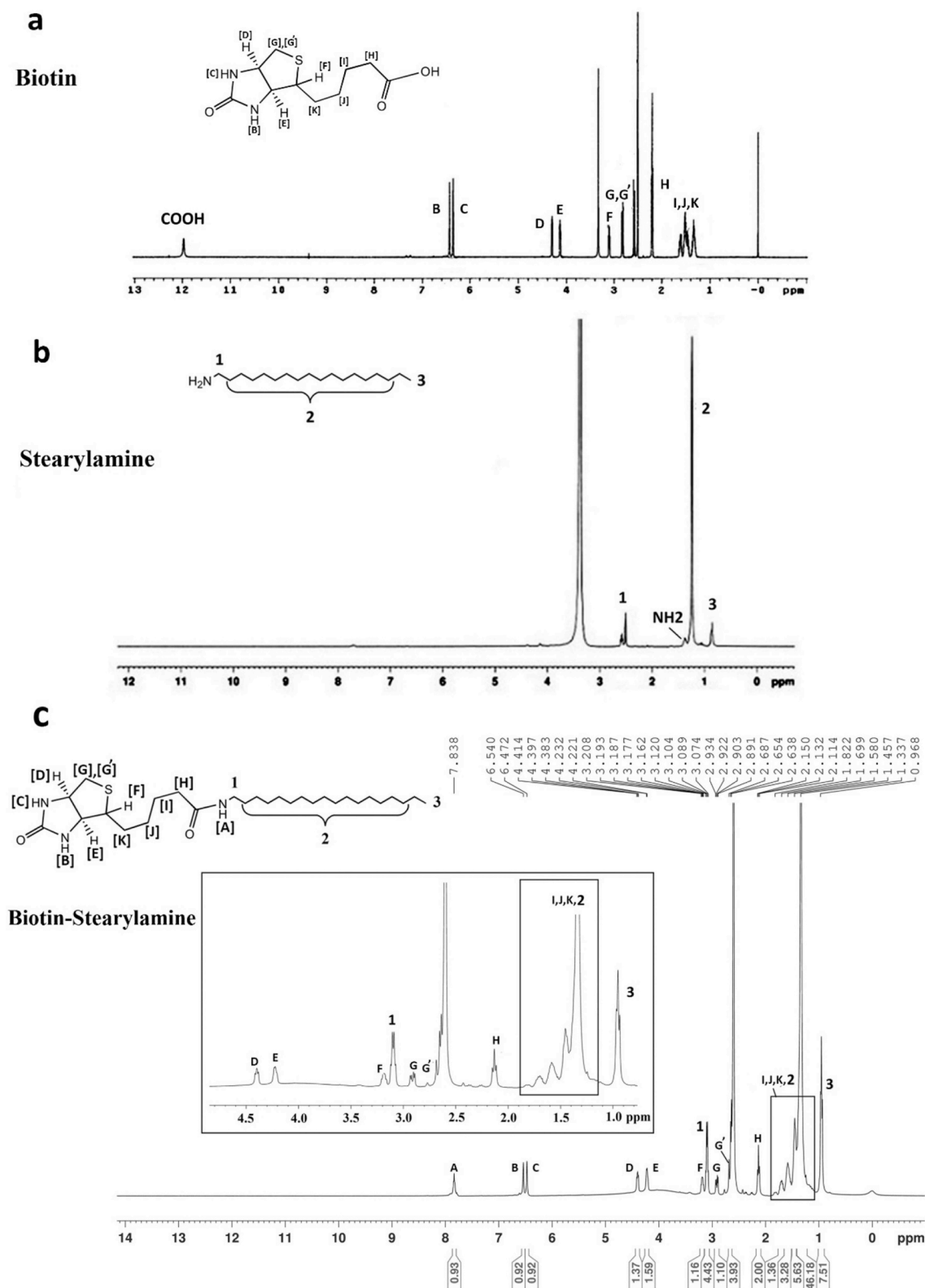Biotin-SUN-NLCs were prepared using the emulsion-solvent

Fig. 1. ^{1}H NMR spectra of (A) Biotin (B), stearylamine and (C) Biotin-stearylamine conjugate.

diffusion and evaporation method. Irregular factorial design was employed to evaluate the effect of several formulation parameters and their interactions on properties of biotin-SUN-NLCs. A number of NP formulations were prepared and the basic characteristics of the products such as particle size, PdI, zeta potential, EE, and RE$_8$% were determined (Table 3). Percent contribution of each variable on SUN EE, particle size, zeta potential and RE$_8$% in biotin-SUN-NLCs is also depicted in Fig. 3. The one factor graphs plotted by Design-Expert software are shown in Figs. 4–8. In each graph, the effect of one variable was investigated while other factors were in its middle level value.
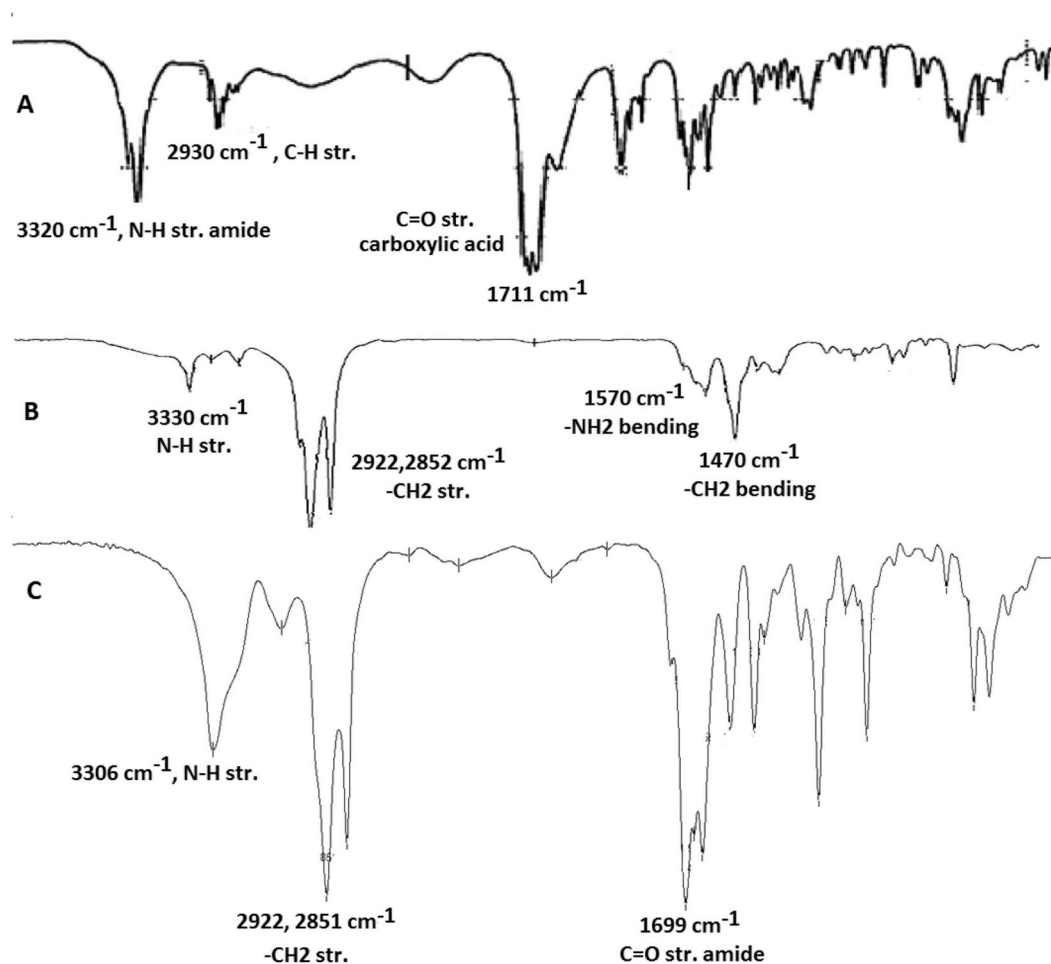
Fig. 2. FTIR of (A) Biotin (B), stearylamine and (C) Biotin-stearylamine conjugate.

Table 3
Physical properties of different SUN loaded biotin modified NLCs.

Formulations	Drug loading efficiency%	Particle size (nm)	Zeta potential, (mV)	PdI	Release efficiency,RE_8%
D5O5L15S0.5	91.42 ± 0.18	192.13 ± 3.5	0.96 ± 0.32	0.16 ± 0.07	43.28 ± 8.45
D10O5L15S0.5	**85.10 ± 2.05**	**125.5 ± 5.26**	**10.23 ± 0.62**	**0.22 ± 0.04**	**62.85 ± 5.46**
D10O10L15S0.5	83.00 ± 1.07	203.2 ± 8.70	6.38 ± 0.46	0.14 ± 0.04	34.88 ± 0.95
D5O5L30S0.5	90.09 ± 2.01	256.23 ± 24.7	6.30 ± 0.38	0.30 ± 0.08	28.84 ± 1.24
D5O10L30S0.5	92.02 ± 0.81	300.53 ± 15.81	8.30 ± 1.00	0.49 ± 0.12	40.35 ± 4.50
D10O10L30S0.5	83.3 ± 2.64	270.80 ± 14.13	10.72 ± 1.52	0.54 ± 0.12	35.58 ± 1.73
D5O10L15S1	89.41 ± 0.50	202.00 ± 12.14	2.94 ± 0.28	0.64 ± 0.33	40.40 ± 4.22
D10O5L15S1	77.19 ± 2.99	216.36 ± 4.53	10.22 ± 1.01	0.12 ± 0.05	64.47 ± 1.62
D10O10L15S1	67.28 ± 5.42	168.66 ± 8.26	13.56 ± 2.33	0.51 ± 0.04	35.90 ± 3.84
D5O5L30S1	91.32 ± 0.54	410.63 ± 56.8	2.44 ± 0.14	0.46 ± 0.14	36.53 ± 2.30
D5O10L30S1	88.71 ± 3.01	353.4 ± 17.20	6.72 ± 0.79	0.46 ± 0.11	46.01 ± 3.049
D10O5L30S1	81.73 ± 1.12	158 ± 18.18	17.33 ± 0.60	0.51 ± 0.01	35.58 ± 2.45

D: Lipid/Drug ratio O: Aqueous/organic phase ratio L: Labrafac/lipid ratio S: Pluronic F127(%).

3.3. Particle size

Particle size is the most important characteristic of NPs determining the amount of drug delivered to the tumor tissue through EPR effect. The size of pores in tumor vasculature endothelium is tumor-dependent ranging between 0.2 and 2 μm, but in the majority of tumors, pore cut-off sizes is about 380–780 nm. Based on the literature review, NPs with a size less than 400 nm are ideal from the perspective of EPR. However, particles smaller than 200 nm are required to get long circulation time and prevent the removal of NPs from blood circulation by reticuloendothelial system (RES) [10]. As depicted in Table 3, the mean values of particle size of biotin-SUN-NLCs were in range of 125.5–410.63 nm. Design of experiment (DOE) result indicates surfactant concentration (%), lipid/drug weight ratio, liquid lipid to total lipid ratio and interaction between of each two pairs of factors have significant effect on the particle size of NPs. The effect of each parameter on resulted particle size is given below:

Particle size = +230.02 + 32.95 A + 4.55 B − 47.79 C + 28.09 D − 28.37 AB − 21.28 AC + 32.02 BC + 26.66 BD − 24.29 CD
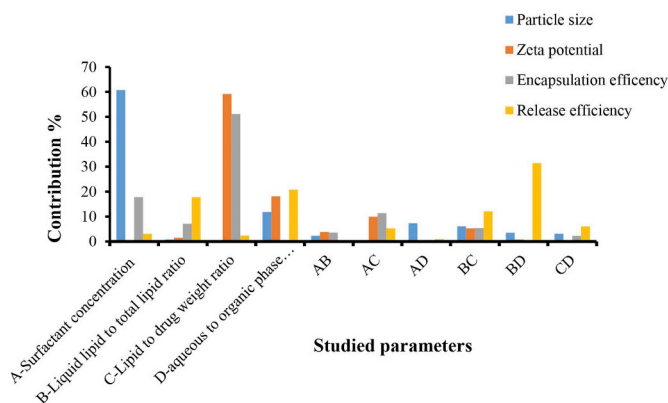
Fig. 3. Contribution of different studied parameters on particle size, zeta potential, encapsulation efficiency and release efficiency of biotin-SUN-NLCs.

$$(4)$$

Where A, B, C and D are surfactant concentration (%), liquid lipid to total lipid ratio (w/w), lipid/drug ratio (w/w), aqueous/organic phase volume ratio, respectively.

Statistical analysis using Design Expert Software showed the most effective factor on the particle size is surfactant concentration (Fig. 3). According to Fig. 4a, by increasing PF127 concentration from 0.5% to 1%, particle size increased. This could be due to particle aggregation induced by increasing the medium viscosity which accompanies increasing PF127 concentrations. Furthermore, employing higher concentration of PF127 reduced the mixing speed during preparation which in turn caused formation of larger NPs [11]. Emami et al. [12] also observed that increasing emulsifier concentration from 0.25 to 0.5% decreased particle size, However, increasing emulsifier concentration more than 0.5% in the formulation resulted in a significant increase in particle size. As it can be seen in Fig. 4b, increasing lipid/drug weight ratio from level 1 to level 2 (decreasing drug content) significantly decreased particle size. This finding is in accordance with other investigations such as those conducted by Fathi and coworkers [13] who reported increasing in size with incorporating higher amount of hesperetin. This was explained with massive physical structure of hesperetin which occupied a huge volume of NPs. The ratio of liquid lipid to total lipid also significantly contributed on particle size. Increment of labrafac content increased mobility of the internal lipids and fluidity of the surfactant layer which in turn increased particle size (Fig. 4c). This observation is well correlated to Das et al. [14] study, who demonstrated that enhancing percentage of liquid lipid increased the particle size of clotrimazole loaded NLCs. PdI is the parameter that gave us information about homogeneity of nanosuspension. The PdI is dimensionless number ranged from 0 to 1. A small value of PdI, usually less than 0.3, indicates that dispersion is monodisperse [15]. As depicted in Table 3, PdI was fluctuating between 0.12 and 0.64. Statistical analysis using Design Expert Software showed that none of studied factors significantly contributed on the PdI of biotin-SUN-NLCs.

3.4. Encapsulation efficiency

EE of biotin-SUN-NLCs varied between 67.28 and 92.02. Equation (5) can be used to accurately predict EE of particles:

$$EE = +85.40 - 2.99\,A - 1.89\,B - 5.85\,C + 0.35\,D - 1.54\,AB - 2.39\,AC - 1.64\,BC + 1.06\,CD \qquad (5)$$

As indicated in Fig. 3, EE was mostly influenced by lipid/drug weight ratio. Increment of drug content significantly increased EE (Fig. 5a) possibly due to good entrapment of drug in the lipids [9]. Surfactant content and aqueous/organic phase volume ratio and
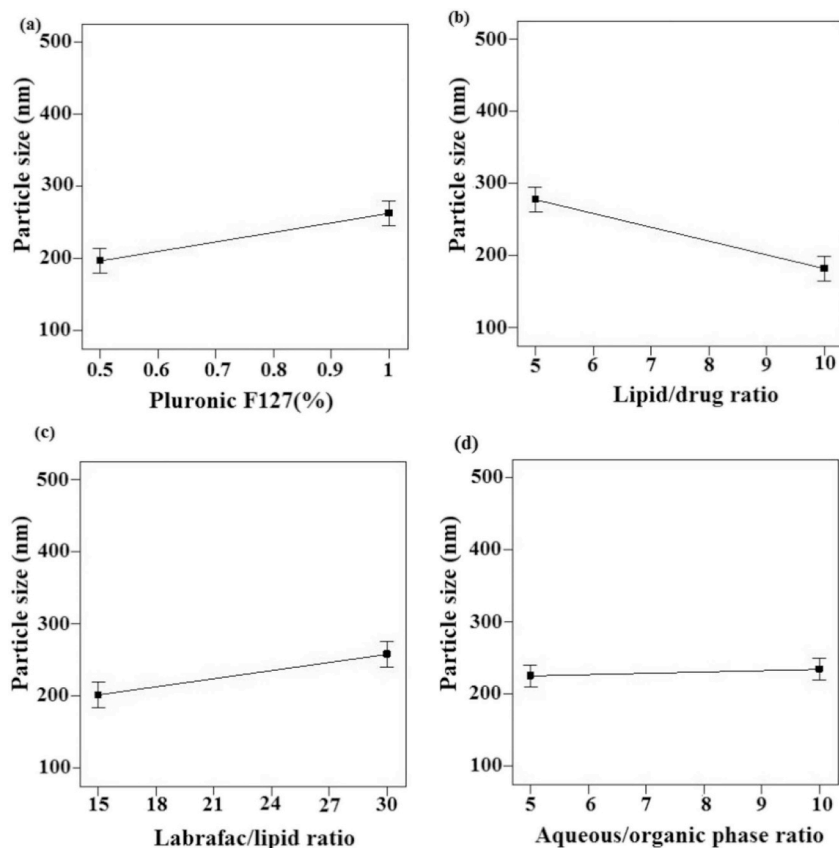

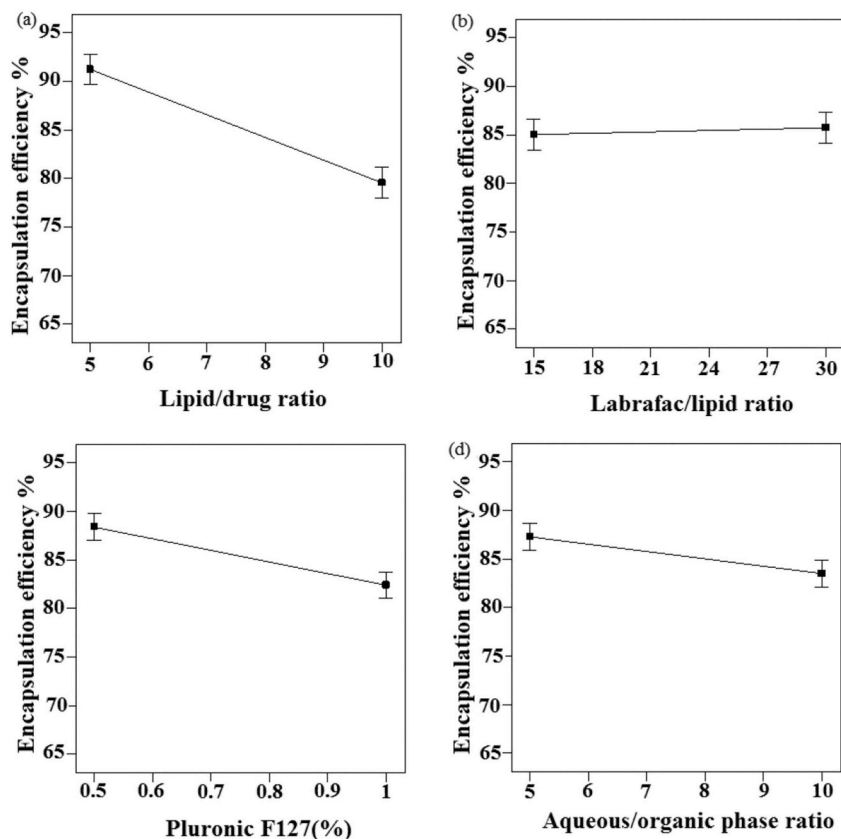**Fig. 4.** Effects of different studied parameters on particle size of biotin-SUN-NLCs.

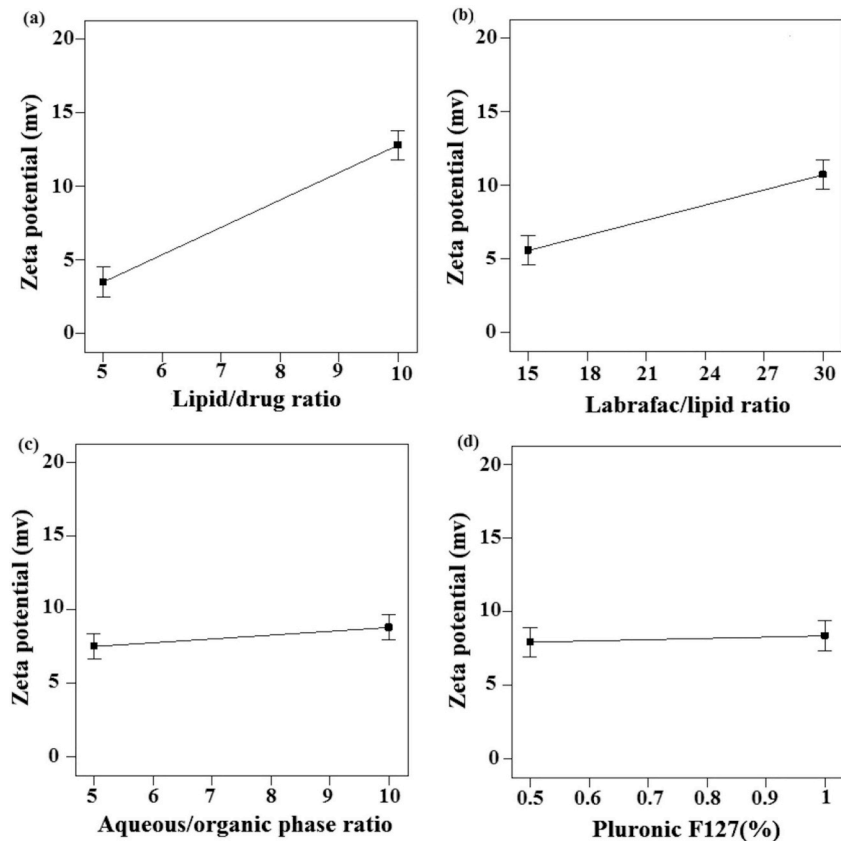Fig. 5. The effects of different studied parameters on encapsulation efficiency of biotin-SUN-NLCs.

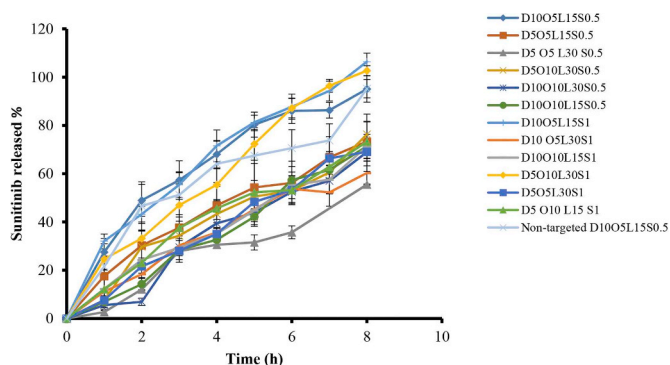Fig. 6. The effects of different studied parameters on zeta potential of biotin-SUN-NLCs.

Fig. 7. SUN release profiles from each studied formulation of biotin-SUN-NLCs.

interaction between of each two pairs of factors were also significantly affecting EE. EE decreased with increasing surfactant concentration (Fig. 5c) probably due to increase in the solubility of SUN in the aqueous phase owing to the solubilization effect of the emulsifier [16]. Increasing aqueous/organic phase ratio also decreased the EE (Fig. 5d). This could be attributed to rapid diffusion of the organic solvent molecules in water and subsequently fast partitioning of the drug molecules into the aqueous phase before the droplet hardening occurred [17]. This finding was in accordance with the previous study of Varshosaz et al. [18] who showed a decrease in valproic acid EE with increasing aqueous/organic phase ratio.

3.5. Zeta potential

Zeta potential is the electric charge at the surface of particle and considered as a key factor to evaluate the physical stability of colloidal suspensions or emulsions. Particle aggregation is less likely to occur for charged particles due to electric repulsion. It is known that zeta potential between ± 5 and 15 mV are in the region of limited flocculation. Steric hindrance provided by sterically stabilizing surfactants such as non-ionic surfactants also impact on particle stability. When the surfactants are employed, even lower zeta potential value is sufficient to ensure good colloidal stability [19]. As depicted in Table 3, the zeta potential values of biotin-SUN-NLCs were positive and varied from 0.96 to 17.33. The positive charges on particles originated from projection of amino groups of B-SA conjugates on the outer surface of the NLCs exposed to the external phase. The following equation shows the effect of each studied factor on zeta potential.

$$\text{Zeta potential} = +8.01 + 0.22A + 0.65B + 4.65C + 2.57D + 1.18AB + 1.65AC - 1.39BC - 0.54BD \qquad (6)$$

Analysis of zeta potential data revealed that the lipid/drug weight ratio is the most effective ($p < 0.05$) variable on zeta potential of the NPs (Fig. 3). DOE result indicated drug content, liquid lipid to total lipid ratio, surfactant concentration in interaction with aqueous/organic phase volume ratio or drug content, aqueous/organic phase volume ratio in interaction with drug content had significant effect on the zeta potential of NLCs. As shown in Fig. 6a, zeta potential value decreased when drug content in NLC was increased. As described earlier, increasing drug content increased the particle size of biotin-SUN-NLCs. The bigger particle size owned the lower charge density which might be the result of smaller surface-to-volume area of larger particles [20]. The zeta potential was also strongly influenced by the liquid lipid to total lipid ratio. It is evident from Fig. 6b, zeta potential increased with increasing liquid lipid to total lipid ratio. This could be related to change in the crystalline structure and crystalline re-orientation of the lipid. Given that different sides of a crystal can possess a different charge density, variation in the crystalline structure and crystalline re-orientation of the lipid may be led to change charges on the particle surface [21].
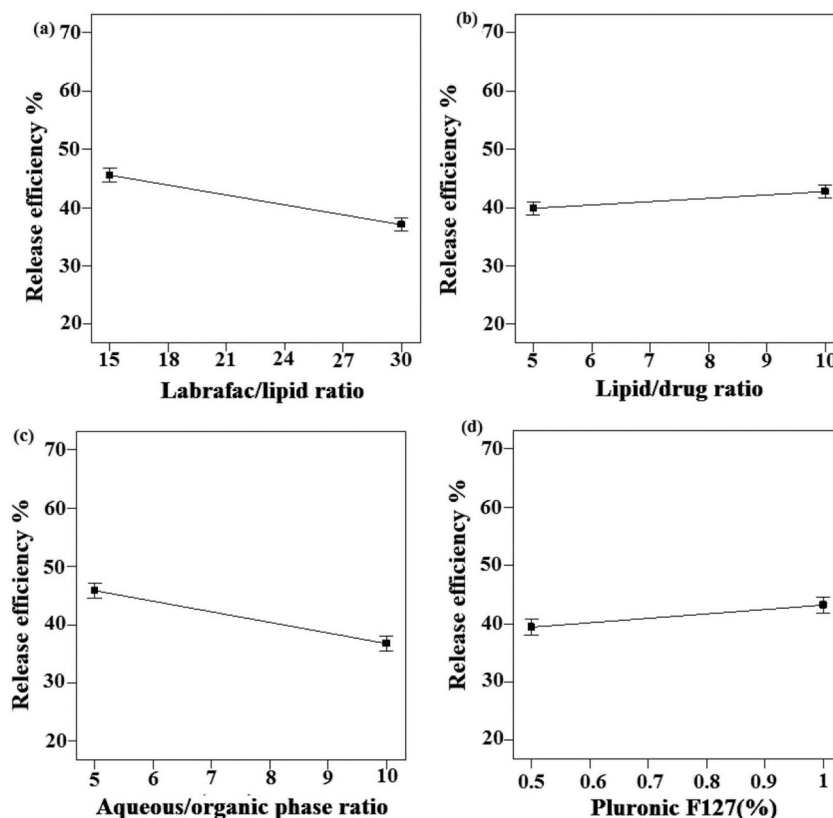

Fig. 8. The effects of different studied parameters on release efficiency of biotin-SUN-NLCs.

3.6. In vitro drug release

Fig. 7 shows the drug release profiles for each studied formulation. To compare release profiles, $RE_8\%$ was calculated. Based on investigated results, the range of $RE_8\%$ was 28.84–64.47%. Fig. 3 shows the most effective parameter on $RE_8\%$ was interaction of liquid lipid/total lipid ratio and aqueous/organic phase volume ratio. Except the interaction of surfactant concentration and liquid lipid/total lipid ratio that did not have significant effect on the $RE_8\%$, other main variables and their interaction had significant effect on this parameter. The following equation shows the effect of each studied factor on $RE_8\%$.

$$RE = +41.32 + 1.90\,A - 4.55\,B + 1.44\,C - 4.26\,D - 2.48\,AC - 1.04\,AD - 3.74\,BC + 6.05\,BD - 2.30\,CD \quad (7)$$

As can be seen in Fig. 8a,b&c, $RE_8\%$ decreased when drug content, labrafac/lipid ratio as well as organic/aqueous phase ratio increased ($P < 0.05$). These changes also increased particle size. Larger particles showed slower rate of drug release owning to decrease surface area of NPs and increase length of the diffusion path that the drug had to travel to reach dissolution medium. Taymouri and co-workers [20] also found that reduction in particle size of nanomicelles increased release rate of docetaxel. It can be seen from Fig. 8d, increasing in PF127 concentration in the external aqueous phase caused an increase $RE_8\%$ owing to the solubilization effect of the emulsifier.

3.7. Optimization

The desirability function was determined using Design Expert Software to achieve the optimized formulation. The optimum formulation was based on the set criteria of maximum EE, maximum zeta potential, minimum particle size, minimum PdI and $RE_8\%$ in the range. Based on the modeling generated by Design Expert Software, the optimized formulation suggested by desirability of 75% was D10O5L15S0.5 that was prepared using 6 mg SUN, 45 mg Chol, 9 mg labrafac and 6 mg B-SA conjugate when the surfactant level was almost 0.5% and the aqueous/organic phase ratio was 5. The optimized formulation exhibited a particle size of 125.50 nm, EE of 85.10%, zeta potential of 10.23 mV, drug release efficiency of about 62.85% during 8 h and PdI of 0.22. As it can be seen in Fig. 9, optimized biotin-SUN-NLCs were spherical with smooth surface. To evaluate the release kinetics and mechanism of release from optimized biotin-NLCs, SUN release data was studied by best curve fitting with different kinetic models such as Higuchi, Baker-lonsdale, first order, zero order and Korsmeyer-Peppas model. Considering the highest correlation coefficient, SUN release kinetics from optimized biotin-NLCs followed Higuchi model ($R^2 = 0.9805$). The slopes obtained from the Korsmeier-

Peppas model was found to 0.5783 indicating that the release was mainly controlled by diffusion coupled with erosion (anomalous diffusion mechanism). SUN loaded non-targeted optimized formulation (non-targeted D10O5L15S0.5) was also developed by replacing B-SA conjugates with Chol as described in section 2.3. The characteristics of non-targeted ones are summarized in Table 4. The release profile of the drug from non-targeted NLCs was shown in Fig. 7. The slightly faster release of drug from targeted D10O5L15S0.5 could be related to smaller particle size of these NPs compared to non-targeted ones. As particle sized decreased, the contacting surface area of NPs increased and the length of diffusion path decreased. As a result, the release rate drug increased [20].

3.8. Cell viability assay

The cellular toxicities of free SUN, SUN-NLCs and biotin-SUN-NLCs in A549 cells were studied by MTT assay which are known to express high level of biotin [4]. As shown in Fig. 10, the cell suppression of all drug loaded NLCs and free SUN increased in dose dependent manner, in which biotin-SUN-NLCs had the highest cell cytotoxicity compared to SUN-NLCs and free SUN. The increased cytotoxicity of biotin-SUN-NLCs could be attributed to the fact that biotin-SUN-NLCs easily entered into the cells via receptor mediated endocytosis. From the results, SUN-NLCs also caused higher cytotoxicity compared to the free SUN at the same concentration. The results well correlated with previous studies which demonstrated higher cytotoxicity of lipid based NPs entrapping drug compared to free drugs [22,23]. This may be attributed to the efficient adherence of lipid NPs to the cell membrane, internalization inside the cell by endocytosis and enhance intracellular drug accumulation.

The IC_{50} values of free SUN, SUN-NLCs, and biotin-SUN-NLCs in A549 cells were 3.14, 2.17, and 1.66 μg/mL, respectively, which exhibited better cellular cytotoxicity of biotin-SUN-NLCs in A549 cells. A similar result was also reported for biotin-decorated pluronic® P123/F127 mixed micelles used for niclosomide delivery compared to the non-targeted micelles and free niclosomide [4].

In addition to biotin-SUN-NLCs and SUN-NLCs, the cytotoxicity of drug free targeted and non-targeted NLCs, in the same concentration as used for drug loaded NLCs was also investigated. As it can be seen in Fig. 10, at low concentrations, the drug free non-targeted NLCs showed negligible toxicity towards A549 cells, but at higher concentrations, a little toxicity was seen with cell viability of near 70%. Drug free targeted NLCs showed higher cytotoxicity than non-targeted ones due to projection of positively charged B-SA conjugates on the surface of the NLCs [24]. In agreement with our study, the study conducted by Varshosaz et al. [25] also showed that positively charged blank NLCs had cytotoxic effects on K562 cells. This phenomenon may be also involved
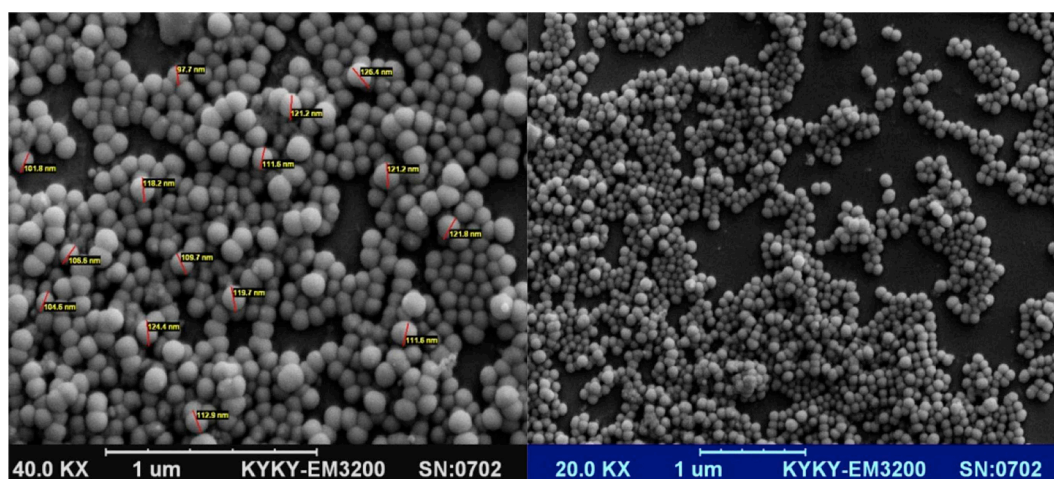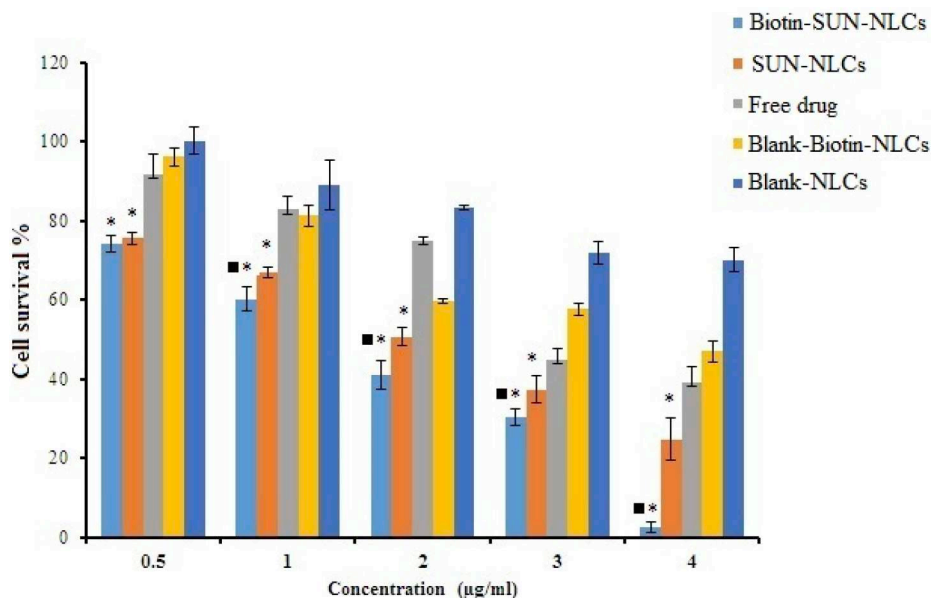

Fig. 9. SEM images of optimized biotin-SUN-NLCs.

Table 4
Physical properties of SUN loaded targeted NLCs and non-targeted ones.

Formulations	Drug loading efficiency%	Particle size (nm)	Zeta potential, (mV)	PDI	Release efficiency, RE_8%
Non-targeted D10O5L15S0.5	78.56 ± 1.98	238.00 ± 6.92	−9.29 ± 0.46	0.21 ± 0.01	55.24 ± 9.23
Targeted D10O5L15S0.5	85.10 ± 2.05	125.5 ± 5.26	10.23 ± 0.62	0.22 ± 0.04	62.85 ± 5.46


Fig. 10. In vitro cellular toxicities of free SUN, SUN-NLCs and biotin-SUN-NLCs in A549 cells after 48 h incubation. $*p < 0.05$ vs. free drug, ■$p < 0.05$ vs. SUN-NLCs.

in higher toxicity of biotin-SUN-NLCs in comparison with SUN-NLCs and free SUN. To compensate impaired safety of these nanocarriers, increment of drug loading % or biotinylation of other fat soluble chemicals such as cholesterol is needed.

3.9. Cellular uptake assay

For investigating the cellular uptake of developed NLCs, both biotin-NLCs and NLCs were loaded with C6. C6 is an efficient compound commonly used as a fluorescent probe for cellular uptake investigation due to its unique properties such as high fluorescent intensity and small leakage rate from NPs formulation [10]. Flow cytometry demonstrated enhanced uptake of biotin-C6-NLCs by A549 cell compared with C6-NLCs. Based on the geometric means of each histogram in Fig. 11, A549 cells treated with biotin-C6-NLCs exhibited higher fluorescence intensity than C6-NLCs, indicating that biotin decoration on particle surface could considerably facilitate the uptake of NLCs by A549 cells via receptor mediated endocytosis. Fluorescent microscope further
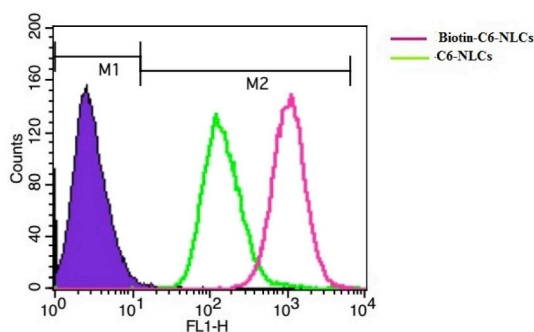
Fig. 11. Flow cytometry profiles of A549 cell line after 3 h of incubation with biotin-C6-NLCs and C6-NLCs.
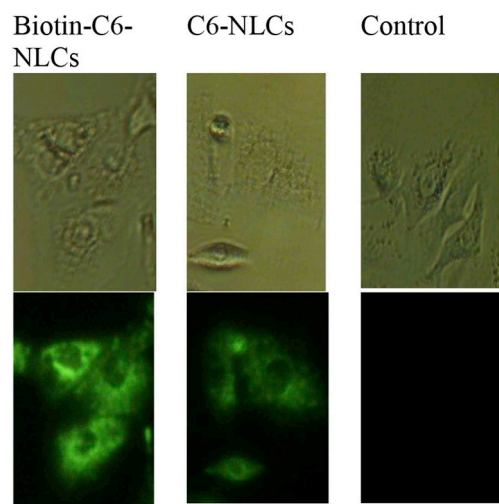
Fig. 12. Fluorescence microscopic images of A549 cells after 3 h incubation with biotin-C6-NLCs and C6-NLCs.

confirmed efficient cellular uptake of biotin-NLCs. As it can be seen in Fig. 12, the fluorescent intensity of biotin-NLCs related to the C6 that entered into cells is more than that of the non-targeted NLCs.

4. Conclusions

In present study, we developed biotin functionalized NLCs for the SUN delivery. B-SA conjugate was synthesized and confirmed by FTIR and H NMR. The formulation variables were optimized using Design Expert Software. The optimized biotin-SUN-NLCs showed acceptable particle sizes with narrow size distributions. Besides, biotin-SUN-NLCs

showed significantly higher cytotoxic effect in lung cancer A549 cells overexpressing biotin receptor compared to that of non-targeted NLCs and free SUN. The improvement of cellular uptake of biotin-SUN-NLCs into A549 cells was also demonstrated. Taken together, biotin-SUN-NLCs can be used as an efficient targeted chemotherapy to cure a number of cancers overexpressing biotin receptors, including lung cancer. However, further study is required to confirm the therapeutic potential of biotin-SUN-NLCs in cancer therapy *in vivo*.

Declaration of conflicting interests

The authors report no conflicts of interest.

Acknowledgments

References

[1] L.G. Paz-Ares, M. Pérol, T.E. Ciuleanu, R.D. Kowalyszyn, M. Reck, C.R. Lewanski, K. Syrigos, O. Arrieta, K. Prabhash, K. Park, J. Pikiel, Treatment outcomes by histology in REVEL: a randomized phase III trial of Ramucirumab plus docetaxel for advanced non-small cell lung cancer, Lung Canc. 112 (2017) 126–133.

[2] S. Tran, P.J. DeGiovanni, B. Piel, P. Rai, Cancer nanomedicine: a review of recent success in drug delivery, Clin. Transl. Med. 6 (2017) 44.

[3] D. Liu, Z. Liu, L. Wang, C. Zhang, N. Zhang, Nanostructured lipid carriers as novel carrier for parenteral delivery of docetaxel, Colloids Surfaces B Biointerfaces 85 (2011) 262–269.

[4] A. Russo, D.S. Pellosi, V. Pagliara, M.R. Milone, B. Pucci, W. Caetano, N. Hioka, A. Budillon, F. Ungaro, G. Russo, F. Quaglia, Biotin-targeted Pluronic® P123/F127 mixed micelles delivering niclosamide: a repositioning strategy to treat drug-resistant lung cancer cells, Int. J. Pharm. 511 (2016) 127–139.

[5] T. Maldiney, M.U. Kaikkonen, J. Seguin, Q. le Masne de Chermont, M. Bessodes, K.J. Airenne, S. Ylä-Herttuala, D. Scherman, C. Richard, In vitro targeting of avidin-expressing glioma cells with biotinylated persistent luminescence nanoparticles, Bioconjug. Chem. 23 (2012) 472–478.

[6] W.G. Sanders, P.C. Hogrebe, D.W. Grainger, A.K. Cheung, C.M. Terry, A biodegradable perivascular wrap for controlled, local and directed drug delivery, J. Contr. Release 161 (2012) 81–89.

[7] M.A. Socinski, S. Novello, J.R. Brahmer, R. Rosell, J.M. Sanchez, C.P. Belani, R. Govindan, J.N. Atkins, H.H. Gillenwater, C. Pallares, L. Tye, Multicenter, phase II trial of sunitinib in previously treated, advanced non–small-cell lung cancer, J. Clin. Oncol. 26 (2008) 650.

[8] J.J. Joseph, D. Sangeetha, T. Gomathi, Sunitinib loaded chitosan nanoparticles formulation and its evaluation, Int. J. Biol. Macromol. 82 (2016) 952–958.

[9] J. Varshosaz, S. Eskandari, M. Tabakhian, Production and optimization of valproic acid nanostructured lipid carriers by the Taguchi design, Pharmaceut. Dev. Technol.

[10] J. Varshosaz, S. Taymouri, F. Hassanzadeh, S. Haghjooy Javanmard, M. Rostami, Folated synperonic-cholesteryl hemisuccinate polymeric micelles for the targeted delivery of docetaxel in melanoma, BioMed Res. Int. 2015 (2015).

[11] T. Ramasamy, U.S. Khandasami, H. Ruttala, S. Shanmugam, Development of solid lipid nanoparticles enriched hydrogels for topical delivery of anti-fungal agent, Macromol. Res. 20 (2012) 682–692.

[12] J. Emami, M. Rezazadeh, H. Sadeghi, K. Khadivar, Development and optimization of transferrin-conjugated nanostructured lipid carriers for brain delivery of paclitaxel using Box–Behnken design, Pharmaceut. Dev. Technol. 22 (2017) 370–382.

[13] M. Fathi, J. Varshosaz, M. Mohebbi, F. Shahidi, Hesperetin-loaded solid lipid nanoparticles and nanostructure lipid carriers for food fortification: preparation, characterization, and modeling, Food Bioprocess Technol. 6 (2013) 1464–1475.

[14] S. Das, W.K. Ng, R.B. Tan, Are nanostructured lipid carriers (NLCs) better than solid lipid nanoparticles (SLNs): development, characterizations and comparative evaluations of clotrimazole-loaded SLNs and NLCs? Eur. J. Pharm. Sci. 47 (2012) 139–151.

[15] M. Danaei, M. Dehghankhold, S. Ataei, F. Hasanzadeh Davarani, R. Javanmard, A. Dokhani, S. Khorasani, M.R. Mozafari, Impact of particle size and polydispersity index on the clinical applications of lipidic nanocarrier systems, Pharmaceutics 10 (2018) 57.

[16] G. Abdelbary, R.H. Fahmy, Diazepam-loaded solid lipid nanoparticles: design and characterization, AAPS PharmSciTech 10 (2009) 211–219.

[17] N. Sharma, P. Madan, S. Lin, Effect of process and formulation variables on the preparation of parenteral paclitaxel-loaded biodegradable polymeric nanoparticles: a co-surfactant study, Asian J. Pharm. Sci. 11 (2016) 404–416.

[18] J. Varshosaz, S. Eskandari, R. Kennedy, M. Tabbakhian, M. Minaiyan, Factors affecting the production of nanostructure lipid carriers of valproic acid, J. Biomed. Nanotechnol. 9 (2013) 202–212.

[19] V. Teeranachaideekul, E.B. Souto, V.B. Junyaprasert, R.H. Müller, Cetyl palmitate-based NLC for topical delivery of Coenzyme Q 10–Development, physicochemical characterization and in vitro release studies, Eur. J. Pharm. Biopharm. 67 (2007) 141–148.

[20] S. Taymouri, J. Varshosaz, F. Hassanzadeh, S.H. Javanmard, N. Dana, Optimisation of processing variables effective on self-assembly of folate targeted Synpronic-based micelles for docetaxel delivery in melanoma cells, IET Nanobiotechnol. 9 (2015) 306–313.

[21] M. Üner, Preparation, characterization and physico-chemical properties of solid lipid nanoparticles (SLN) and nanostructured lipid carriers (NLC): their benefits as colloidal drug carrier systems, Pharmazie 61 (2006) 375–386.

[22] D. Liu, Z. Liu, L. Wang, C. Zhang, N. Zhang, Nanostructured lipid carriers as novel carrier for parenteral delivery of docetaxel, Colloids Surfaces B Biointerfaces 85 (2011) 262–269.

[23] Z. Shao, Z. Shao, B. Tan, S. Guan, Z. Liu, Z. Zhao, F. He, J. Zhao, Targeted lung cancer therapy: preparation and optimization of transferrin-decorated nanostructured lipid carriers as novel nanomedicine for co-delivery of anticancer drugs and DNA, Int. J. Nanomed. 10 (2015) 1223.

[24] X.Y. Yang, Y.X. Li, M. Li, L. Zhang, L.X. Feng, N. Zhang, Hyaluronic acid-coated nanostructured lipid carriers for targeting paclitaxel to cancer, Cancer Lett. 334 (2013) 338–345.

[25] A. Khajavinia, J. Varshosaz, A.J. Dehkordi, Targeting etoposide to acute myelogenous leukaemia cells using nanostructured lipid carriers coated with transferrin, Nanotechnology 23 (2012) 405101.